福井大学
工学部 研究報告
第41巻 第2号
1993年9月

Two-Dimensional Flow around a Square Cylinder at Low Reynolds Number

— Effects of Channel Side-Wall and Fluid Elasticity —

Motoyoshi TACHIBANA*, Nobuyoshi KAWABATA*, and Chao CHEN*

(Received Aug. 2, 1993)

The present paper deals with two-dimensional flow field around a square cylinder moving slowly with a constant velocity along the central line of channel. The effects of the channel side-wall and the fluid elasticity to the flow field were studied by the flow visualization and the numerical analysis. The expansion of streamlines in the vicinity of the square cylinder is suppressed by the approach of the channel side-wall and the length of twin-vortices in the rear of square cylinder decreases with a decrease of the ratio of the channel breadth to the side length of square cylinder. The fluid elasticity in viscoelastic fluids suppresses the expansion of streamlines in the rear part of the square cylinder and makes rear twin-vortices smaller. Besides, the computational experiments based on Maxwell model were carried out in the ranges of 10-50 of Reynolds number and 0-0.10 of Weissenberg number. It was shown that the length of rear twin-vortices increased with an increase of Reynolds number and decreased with an increase of Weissenberg number.

1. Introduction

The flow around a body has been studied by many researchers as one of classical problems in fluid mechanics. In the case of the flow around a square cylinder, the flow field becomes more complicated than that of a circular cylinder, because of the separation at the front corner, the reattachment to the side surface, the wake in the rear of cylinder and so on. On the other hand, the finite property of flow field is the first consideration in the discussion based on experimental or numerical results. Then, our object was limited to the flow field around the square cylinder set in the central plane parallel to two papallel side-walls. Such a flow field has been studied by Fromm-Harlow[1], Hayashi[2], Matida et al[3], Tachibana[4], Tachibana-Matsumoto[5], Nakabayashi-Aoi[6] and Ohwa et al[7] and they have clarified several characteristics of Poiseuille flow and uniform flow around the square cylinder. The fluid used in those papers was Newtonian fluid. If the fluid is viscoelastic fluid, it seems that there are some anomalous phenomena[8]. So that we study the effects of the channel side-wall and the fluid elasticity to above-mentioned flow field in the range of Re=10~50 (the twin-vortices region).

*Dept. of Mech. Eng.

Nomenclature

B:	side length of square cylinder
H:	width of flow field between two papallel planes
L:	length of twin-vortices in the rear of square cylinder
U:	constant velocity of square cylinder
Pc:	concentration of dilute polymer solution (ppm)
ρ :	fluid density
ν :	fluid kinematic viscosity
μ :	fluid viscosity $\mu = \rho \cdot \nu$
λ:	fluid relaxation time (Maxwell model)
x, y:	non-dimensional values of Cartesian coordinate system, $(x, y) = (X, Y)/B$
t:	non-dimensional value of time, $t = T/(B/U)$
u, v:	non-dimensional values of velocities in Cartesian coordinate system, $(u, v) = (V_x, V_y)/U$
P:	non-dimensional value of pressure, $P = p/\rho U^2$
P_{xx}, P_{yy}, P_{xy}:	non-dimensional values of stress components, $P_{ij} = p_{ij}/\rho U^2$
$\sigma_{xx}, \sigma_{yy}, \sigma_{xy}$:	non-dimensional values of elastic parts of P_{xx}, P_{yy}, P_{xy}
Re:	Reynolds number, $Re = \rho UB/\mu = UB/\nu$
W:	Weissenberg number, $W = \lambda U/B$

2. Experiment

2.1 Apparatus and Procedure

The towing channel used are made of the acrylic resin and its dimension are 700mm in length, 100mm in width and 160mm in depth. The black paint was coated on the surface of two side-walls of channel and a photographic window with 660mm in length and 9mm in width was mounted at 54mm in depth from the top of channel. A partition plate was set between two parallel planes to adjust the width of flow field. In the present experiment, the width of channel was changed as 100mm, 40mm and 20mm to discuss its effect on the flow field.

The square cylinder made by the acrylic resin is 10mm in side length and 145mm in length. It is fixed to the translating stand by the arm made of stainless steel rod of 2.5mm in diameter. The cylinder and the camera mounted together on the stand move slowly at the constant velocity along the central plane of channel. The range of Reynolds number in this experiment is 10~50.

The flow field around the square cylinder was visualized by the tracer method using the aluminium powder. On the basis of recording photographs, the flow pattern around the cylinder was discussed and the length of twin-vortices in the rear of cylinder was determined to clarify its dependence upon several governing factors.

2.2 Liquid Used

Liquids used are tap water and dilute polymer solutions. Polymer solutions are aqueous solutions of polyacrylamide (PAA-ZH880H) and the range of polymer concentration is 10~100ppm. The density of polymer solutions was virtually the same as water, i.e. ρ=1000kg/m^3. Besides, as these solutions were dilute ones, we considered ones to be Newtonian fluids[9]. Therefore,

their kinematic viscosity was measured with Ubbelohde viscometer. Their typical values are shown in Table1. From experimental data in past[10–12], it can be considered that polymer solutions used are viscoelastic. But, it is difficult to measure the elasticity of such solutions, because their elasticity is weak and the convenient measuring devices are not existent. Then, we did not measure the elasticity of testing liquids and relatively evaluated the elastic effect of polymer solutions on the viewpoint that the elastic effect of solutions increased with an increase of the polymer concentration.

Table 1 Viscosity of polymer solutions

Kinematic Viscosity ν(mm^2/s)			
Concentration Pc(ppm)	Temperature T(°C)		
	5.0	10.0	15.0
0(water)	1.520	1.310	1.146
10	1.583	1.365	1.183
30	1.719	1.409	1.204
50	1.766	1.553	1.293
70	1.913	1.620	1.411
100	2.355	2.001	1.743

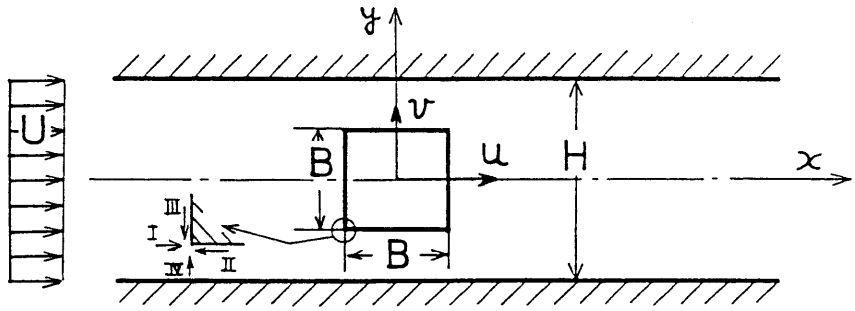

Fig.1 Flow field and coordinate system

3. Numerical Analysis

3.1 Basic Equations

We consider a square cylinder with B in side length moving in -x direction at the constant velocity U along the central plane parallel to two parallel side planes in the two-dimensional channel of H in width. Besides, it is assumed that the fluid in the channel is an incompressible viscoelastic fluid kept in the isothermal state. This flow field is equal to that of the uniform flow moving in x direction around the fixed square cylinder which center is at the origin of Cartesian coordinate system as shown in Fig.1. The governing equations are expressed as:

$$\left.\begin{aligned}\frac{\partial u}{\partial t}+u\frac{\partial u}{\partial x}+v\frac{\partial u}{\partial y}&=-\frac{\partial P}{\partial x}+\frac{\partial P_{xx}}{\partial x}+\frac{\partial P_{xy}}{\partial y}\\ \frac{\partial v}{\partial t}+u\frac{\partial v}{\partial x}+v\frac{\partial v}{\partial y}&=-\frac{\partial P}{\partial y}+\frac{\partial P_{xy}}{\partial x}+\frac{\partial P_{yy}}{\partial y}\end{aligned}\right\} \qquad (1)$$

$$\frac{\partial u}{\partial x}+\frac{\partial v}{\partial y}=0 \qquad (2)$$

And that, as the constitutive equation of viscoelastic fluid, we use Maxwell model(μ=const. λ=const). The relations between stress components are expressed as:

$$\left.\begin{aligned}P_{xx}+W\left(\frac{\partial P_{xx}}{\partial t}+u\frac{\partial P_{xx}}{\partial x}+v\frac{\partial P_{xx}}{\partial y}-2\frac{\partial u}{\partial x}P_{xx}-2\frac{\partial u}{\partial y}P_{xy}\right)&=\frac{2}{Re}\frac{\partial u}{\partial x}\\ P_{yy}+W\left(\frac{\partial P_{yy}}{\partial t}+u\frac{\partial P_{yy}}{\partial x}+v\frac{\partial P_{yy}}{\partial y}-2\frac{\partial v}{\partial x}P_{xy}-2\frac{\partial v}{\partial y}P_{yy}\right)&=\frac{2}{Re}\frac{\partial v}{\partial y}\\ P_{xy}+W\left(\frac{\partial P_{xy}}{\partial t}+u\frac{\partial P_{xy}}{\partial x}+v\frac{\partial P_{xy}}{\partial y}-\frac{\partial v}{\partial x}P_{xx}-\frac{\partial u}{\partial y}P_{xx}\right)&=\frac{1}{Re}\left(\frac{\partial u}{\partial y}+\frac{\partial v}{\partial x}\right)\end{aligned}\right\} \qquad (3)$$

where Reynolds number and Weissenberg number are defined as:

$$\left.\begin{aligned}Re&=\frac{\rho UB}{\mu}=\frac{UB}{\nu}\\ W&=\frac{\lambda U}{B}\end{aligned}\right\} \qquad (4)$$

If the stress components are divided as the viscous part and the elastic part σ_{ij}, they can be expressed as:

$$\left.\begin{aligned}P_{xx}&=\sigma_{xx}+\frac{2}{Re}\frac{\partial u}{\partial x}\\ P_{yy}&=\sigma_{yy}+\frac{2}{Re}\frac{\partial v}{\partial y}\\ P_{xy}&=\sigma_{xy}+\frac{1}{Re}\left(\frac{\partial v}{\partial x}+\frac{\partial u}{\partial y}\right)\end{aligned}\right\} \qquad (5)$$

The flow field (u, v, p) is determined by Eqs.(1)~(3) and concurrently stress compoments (P_{xx}, P_{yy}, P_{xy}) are also solved.

The boundary conditions are as follows:

(a) The entrance section of upper reaches:

$$\left.\begin{aligned}&u=1,\ v=0,\ \frac{\partial P}{\partial x}=0\\ &\sigma_{xx}=,\ \sigma_{yy}=0,\ \sigma_{xy}=0\end{aligned}\right\} \qquad (6)$$

(b) The exit section of lower reaches:

$$\left.\begin{aligned} &\frac{\partial u}{\partial x}=0,\ v=0,\ P=0 \\ &\frac{\partial \sigma_{xx}}{\partial x}=0,\ \frac{\partial \sigma_{yy}}{\partial x}=0,\ \frac{\partial \sigma_{xy}}{\partial x}=0 \end{aligned}\right\}. \tag{7}$$

(c) On the side planes:

$$\left.\begin{aligned} &u=1,\ v=0,\ \frac{\partial P}{\partial y}=\frac{\partial P_{xy}}{\partial x}+\frac{\partial P_{yy}}{\partial y} \\ &\frac{\partial^2 \sigma_{xx}}{\partial y^2}=0,\ \frac{\partial^2 \sigma_{yy}}{\partial y^2}=0,\ \frac{\partial^2 \sigma_{xy}}{\partial y^2}=0 \end{aligned}\right\}. \tag{8}$$

(d) On the central plane:

$$\left.\begin{aligned} &\frac{\partial u}{\partial y}=0,\ v=0,\ \frac{\partial P}{\partial y}=0 \\ &\frac{\partial \sigma_{xx}}{\partial y}=0,\ \frac{\partial \sigma_{yy}}{\partial y}=0,\ \sigma_{xy}=0 \end{aligned}\right\}. \tag{9}$$

(e) On the surface of square cylinder:

(e-1) On the side surface parallel to the x axis:

$$\left.\begin{aligned} &u=0,\ v=0,\ \frac{\partial P}{\partial y}=\frac{\partial P_{xy}}{\partial x}+\frac{\partial P_{yy}}{\partial y} \\ &\frac{\partial^2 \sigma_{xx}}{\partial y^2}=0,\ \frac{\partial^2 \sigma_{yy}}{\partial y^2}=0,\ \frac{\partial^2 \sigma_{xy}}{\partial y^2}=0 \end{aligned}\right\}. \tag{10.1}$$

(e-2) On the side surface parallel to the y axis:

$$\left.\begin{aligned} &u=0,\ v=0,\ \frac{\partial P}{\partial x}=\frac{\partial P_{xx}}{\partial x}+\frac{\partial P_{xy}}{\partial y} \\ &\frac{\partial^2 \sigma_{xx}}{\partial x^2}=0,\ \frac{\partial^2 \sigma_{yy}}{\partial x^2}=0,\ \frac{\partial^2 \sigma_{xy}}{\partial x^2}=0 \end{aligned}\right\}. \tag{10.2}$$

(e-3) At the corner:

$$\left.\begin{aligned} &u=0,\ v=0,\ P=\frac{P_{\mathrm{II}}+P_{\mathrm{III}}}{2} \\ &\sigma_{xx}=\frac{\sigma_{xx,\,\mathrm{I}}+\sigma_{xx,\,\mathrm{IV}}}{2},\ \sigma_{yy}=\frac{\sigma_{yy,\,\mathrm{I}}+\sigma_{yy,\,\mathrm{IV}}}{2},\ \sigma_{xy}=\frac{\sigma_{xy,\,\mathrm{I}}+\sigma_{xy,\,\mathrm{IV}}}{2} \end{aligned}\right\}. \tag{10.3}$$

The subscripts I∼IV stand for I∼IV directions to a corner and we consider that the stress value at the corner is equal to the mean value of two stress values at the corner on adjacent side planes at which the 2nd order differential is zero.

3.2 Method of Solution

We apply Euler implicit scheme to time differential of the governing equation (1) and Lax's scheme to time differential of the constitutive equations (3) and (5) and approximate spatial derivatives in these equations with the central difference of 2nd order precision. Basic equations were solved numerically by the time-marching method[13]. Considering the symmetry to the central plane(y=0), the calculation was carried out in the lower half region($-H/2B \leqq y \leqq 0$) of Fig.1. The finite difference mesh was the orthogonal linear mesh divided unequally. We arranged so that there were more grids in the vicinity of the square cylinder and the intervals of grids changed continuously. The details of the region of calculation and the difference mesh are shown in Table 2. The figure 2 shows the typical mesh scheme.

Table 2 Calculating region and difference mesh

(a) Calculating region and grid number

Name	Mesh Coordinates			
	Grid Number	x-Direction	Grid Number	y-Direction
H2-A	1	-5.0	1	-1.0
	41	-0.5	17	-0.5
	60	0.5	31	0
	113	7.25		
H2-B	1	-5.0	1	-1.0
	41	-0.5	17	-0.5
	60	0.5	31	0
	99	5.0		
H4-A	1	-5.0	1	-2.0
	41	-0.5	23	-0.5
	60	0.5	37	0
	113	7.25		
H10-A	1	-5.0	1	-5.0
	41	-0.5	30	-0.5
	60	0.5	44	0
	113	7.25		

(b) Flow condition and difference mesh

Flow Conditions			Mesh Name
H/B	Re	W	
2	10	0	H2-B
	20		H2-B
	30		H2-A
	40		H2-A
	50		H2-A
4	10	0	H4-A
---	20		---
10	30		H10-A
	40		
	50		
2	10	0.01	H2-B
		0.02	
	---	0.05	
	20	0.07	
		0.10	
	30	0.01	H2-A
	---	0.02	H2-A
	40	0.05	H2-A
	---	0.07	H2-A
	50	0.10	H2-B

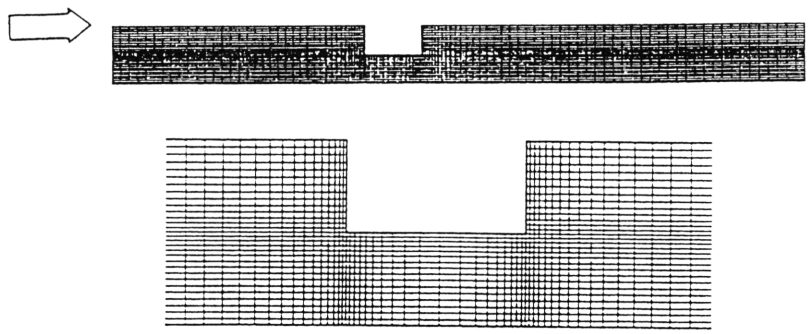

Fig.2 Typical mesh scheme

4. Results and Discussion

4.1 Side-wall Effect

The photographs of the flow around the square cylinder in tap water(Newtonian fluid, Pc=0ppm) are shown in Fig.3 and Fig.4. Fig.3 is of Re=10 and Fig.4 is of Re=50. In

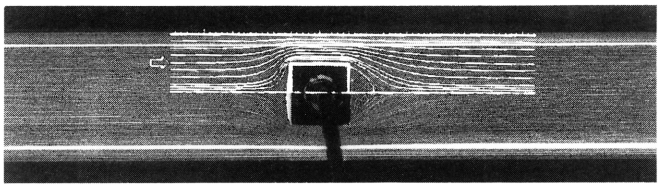

(a) H/B = 2

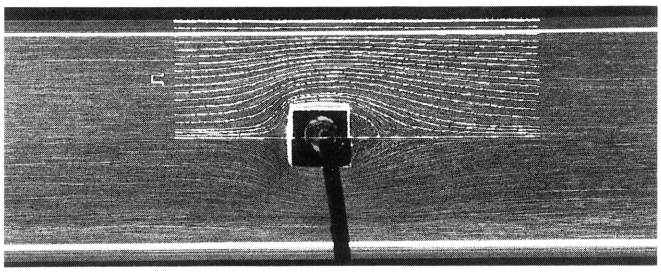

(b) H/B = 4

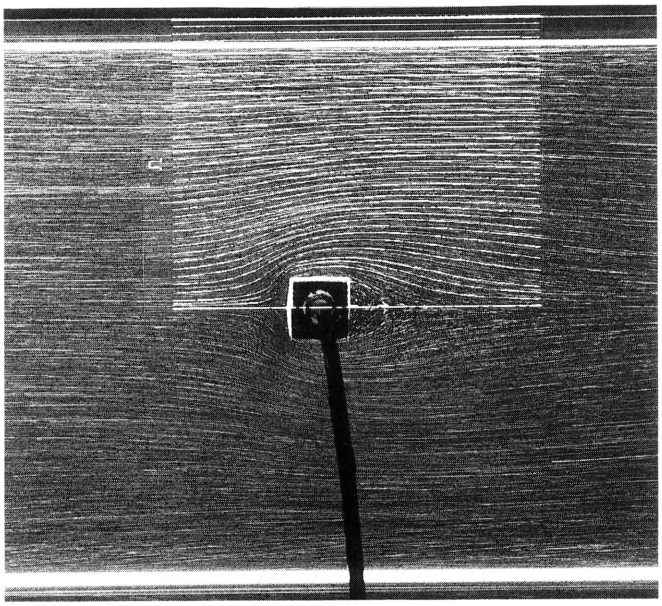

(c) H/B = 10

Fig.3 Effect of channel side-wall to flow field (Re=10)

these figures, results of numerical analysis were transferred in upper half region of each figure. Moreover, in both figures, results of H/B=2,4 and 10 are shown together in order to see the effect of the channel side-wall. From these figures, it is found that (i) experimental results of flow patterns around the square cylinder agree, on the whole, well with numerical results and (ii) the twin-vortices in the rear of square cylinder increases with an increase of Re and decreases with a decrease of H/B. Besides, the size of twin-vortices was discussed on the basis

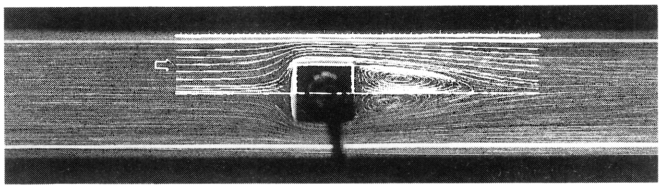

(a) H/B = 2

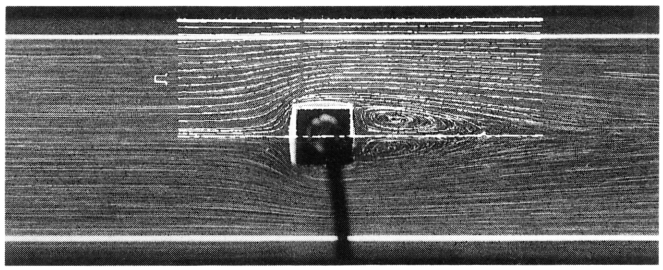

(b) H/B = 4

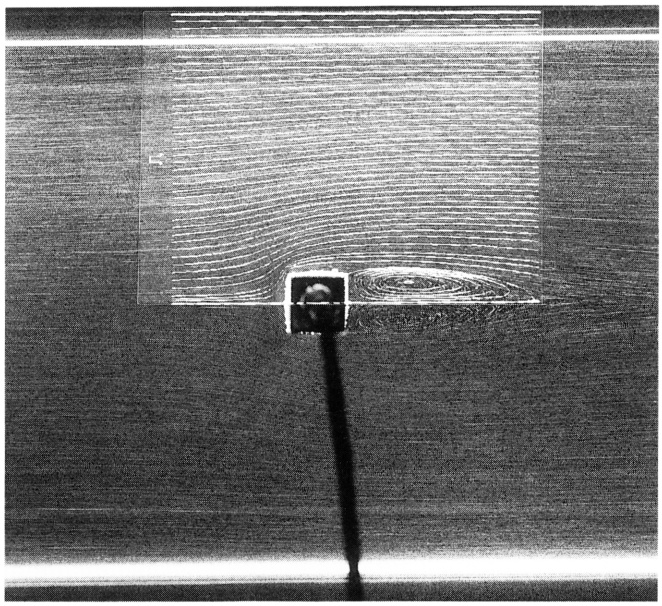

(c) H/B = 10

Fig.4 Effect of channel side-wall to flow field (Re=50)

of its relative length L/B. Fig.5 illustrates the relation between L/B and H/B at different Re. Experimental data were shown by symbolic points and broken lines and numerical results were entered by solid lines. Numerical results are larger than experimental data and its degree reaches to 15~25% of experimental data. The present numerical result was compared with experimental results by Hayashi[2]. It is shown in Fig.6. Our numerical result is also more than his experimental one. It seems that such a difference between the analysis and the experiment is due to the precision of flow visualization and the effect of three-dimensional flow.

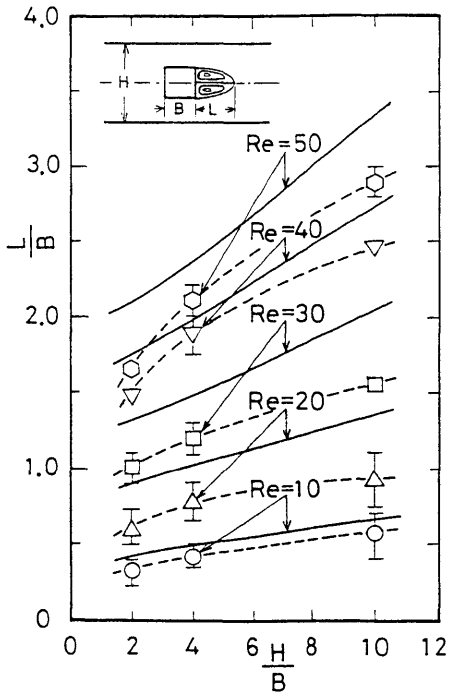

Fig.5 Effect of channel side-wall to length of twin-vortices

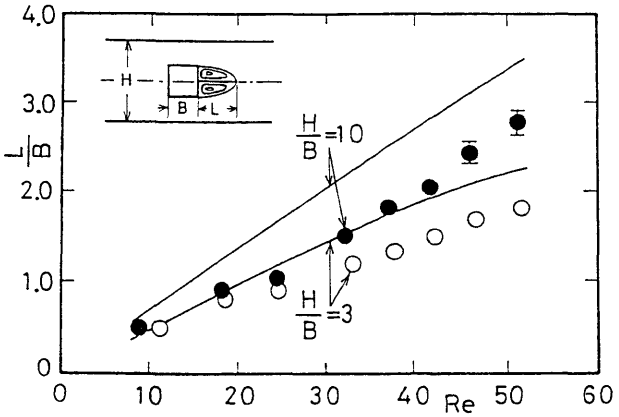

Fig.6 Effect of channel side-wall to length of twin-vortices (M.Hayashi 1972)

4.2 Elasticity Effect

The flow field around the square cylinder in dilute polymer solutions(viscoelastic fluid, Pc=10~100ppm) was discussed in the range of Re=10~50 at H/B=2. Typical results are shown in Fig.7 and Fig.8. In each of these figures, results of numerical simulation for Newtonian fluid(Pc=0ppm) are entered in upper half region together with experimental results. Moreover, the relative length L/B of twin-vortices in the rear of square cylinder was determined for polymer solutions at different Re. Fig.9 shows the relation between L/B and Pc in the range of Re=10~50. From such plottings, we see that (i) the twin-vortices in viscoelastic fluid increases with an increase of Re, which is the same as in Newtonian fluid and (ii) the twin-vortices in viscoelastic fluid decreases with an increase of Pc at same Re. That is, the twin-vortices in the rear of square cylinder increases with the effect of fluid inertia and decreases with the effect of fluid elasticity.

Next, regard dilute polymer solutions as viscoelastic fluids based on Maxwell model, the numerical simulation at H/B=2 was carried out in Re=10~50 and W=0~0.10. A part of results are shown in Figs.10~12. Fig.10 is the streamlines diagram. It shows that in the rear of the square cylinder, the expansion of streamlines are suppressed and the region of twin-vortices decreases with an increase of W which is a parameter of fluid elasticity. To illustrate the effect of fluid elasticity, the typical streamlines were drawn and written together in a figure. From

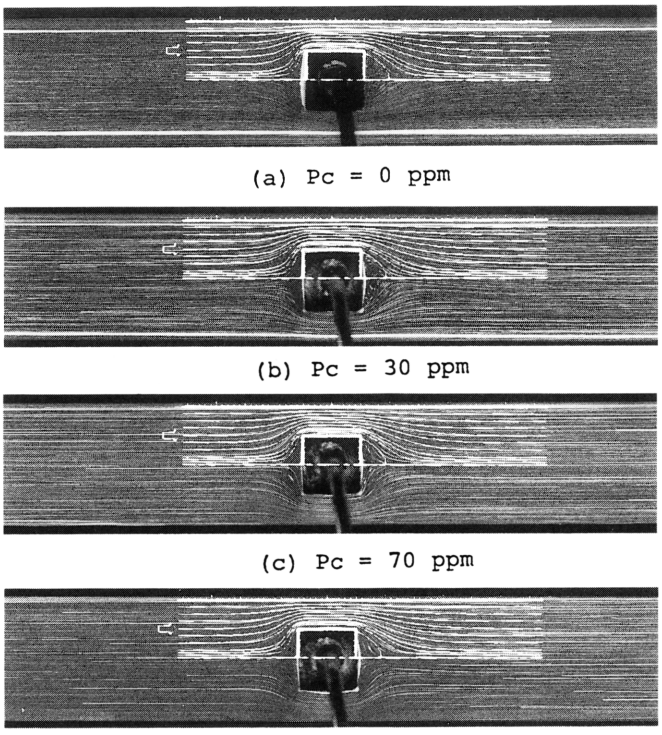

Fig.7 Effect of fluid elasticity to flow field (Re=10)

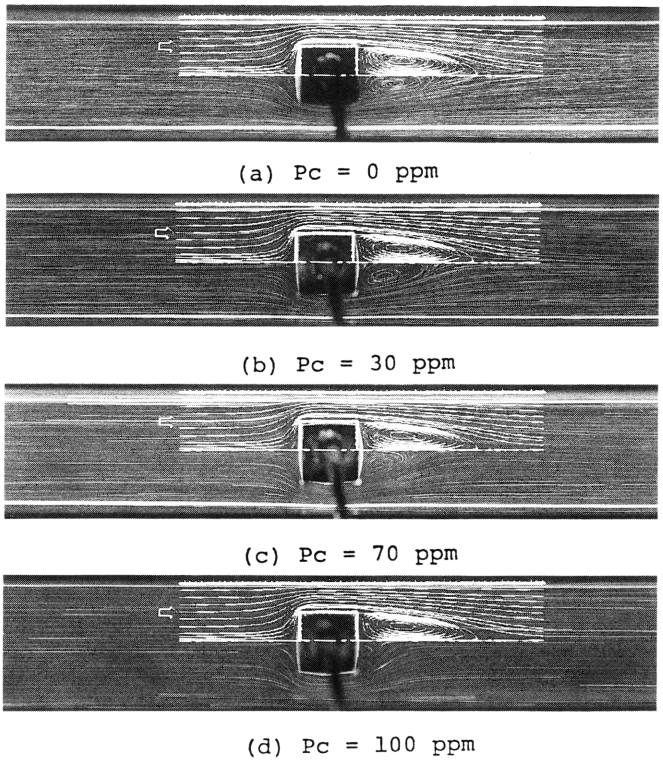

Fig.8 Effect of fluid elasticity to flow field (Re=50)

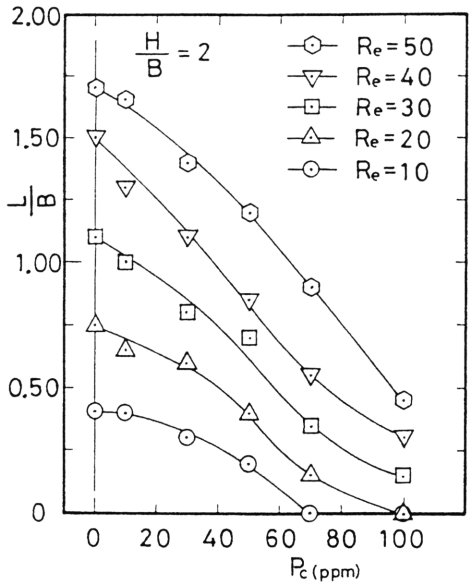

Fig.9 Effect of fluid elasticity to length of twin-vortices

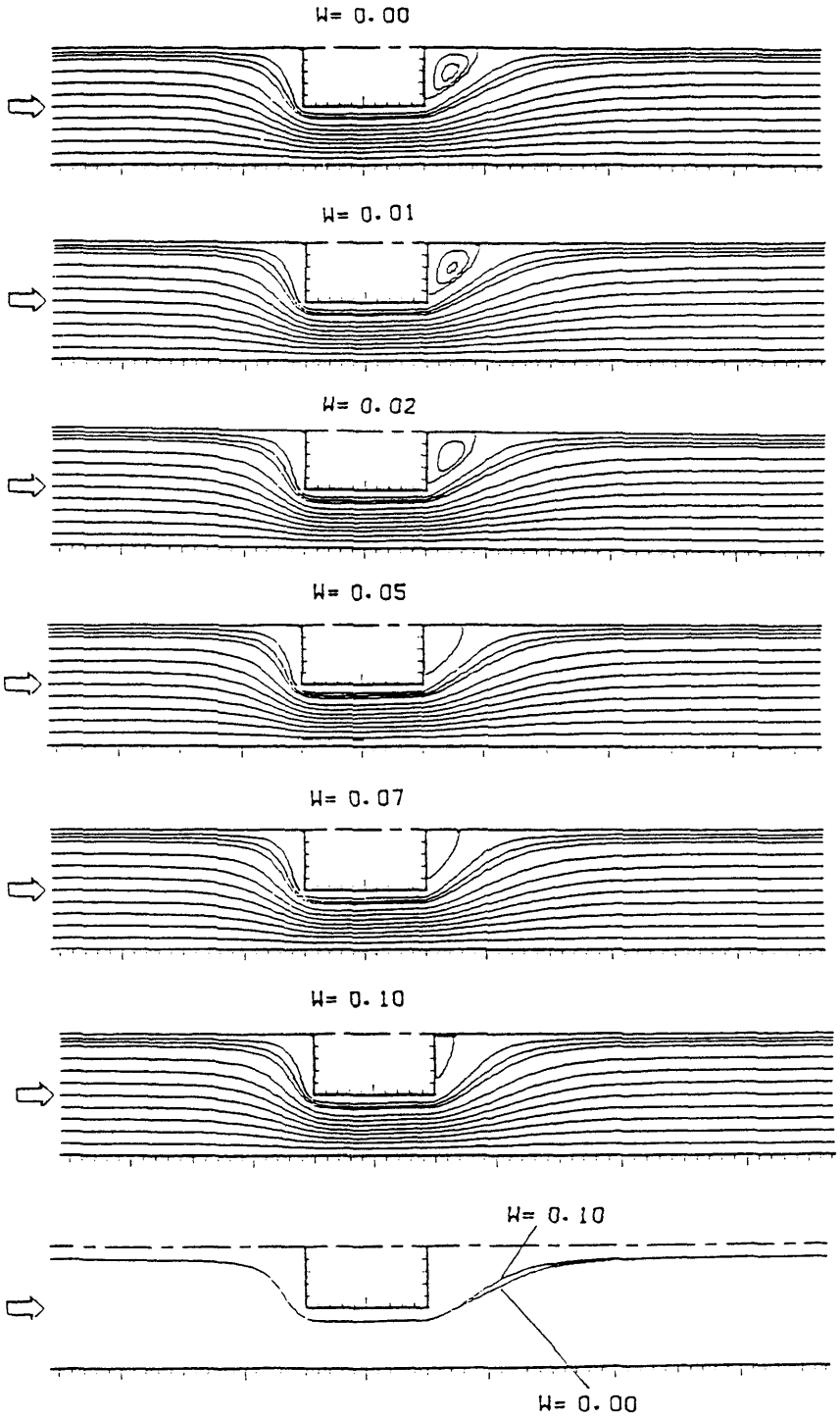

Fig.10a Streamlines in viscoelastic fluids (Re=10)

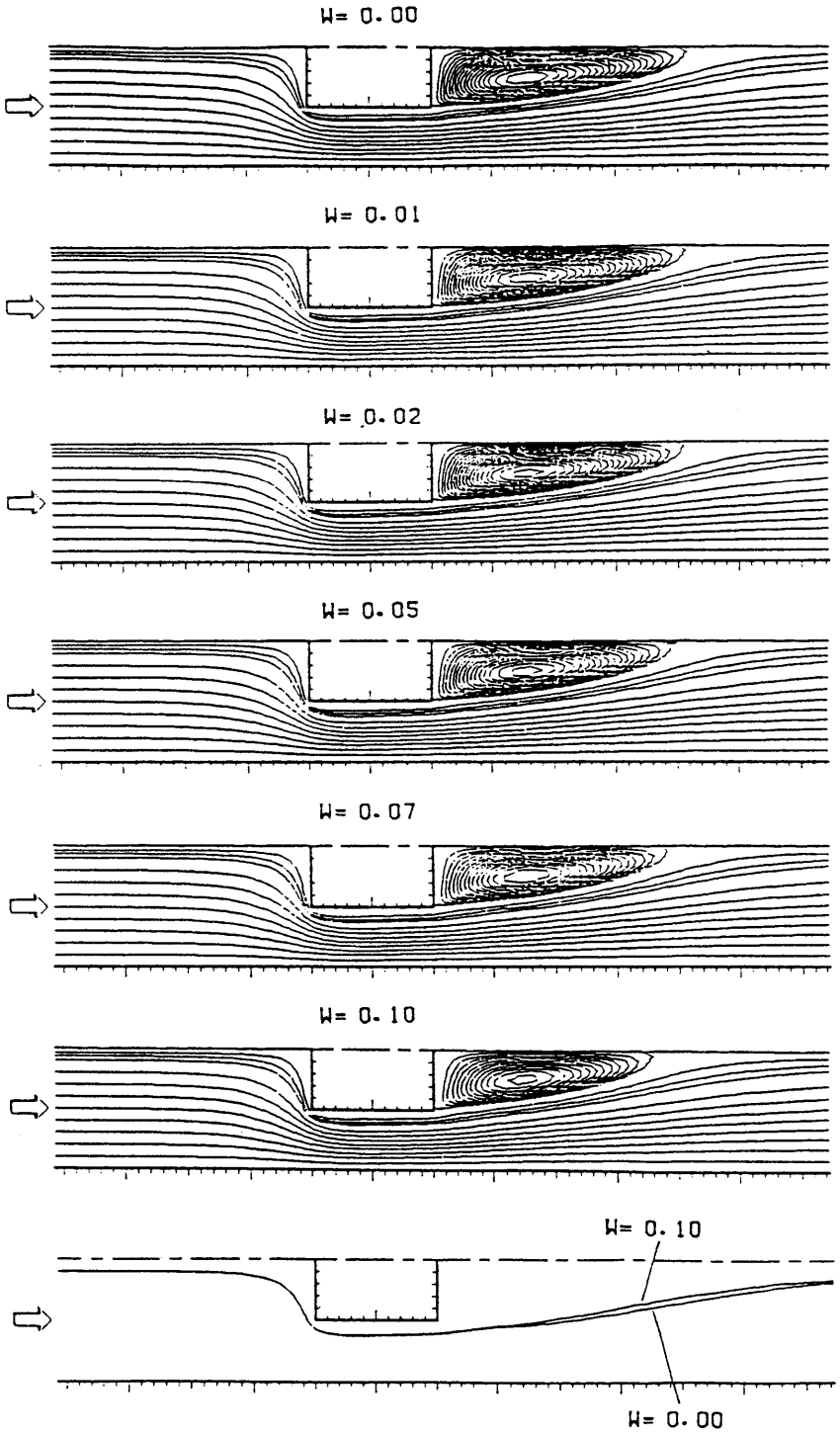

Fig.10b Streamlines in viscoelastic fluids (Re=50)

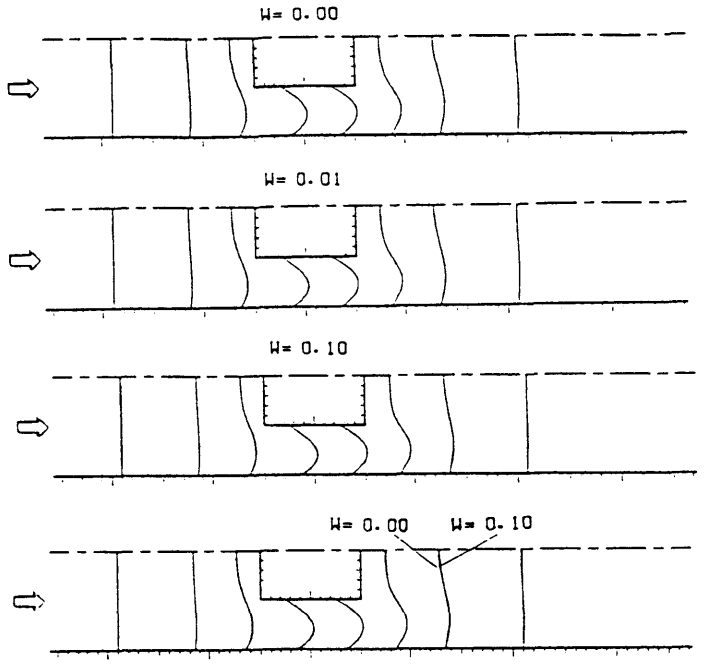

(a) Re = 10

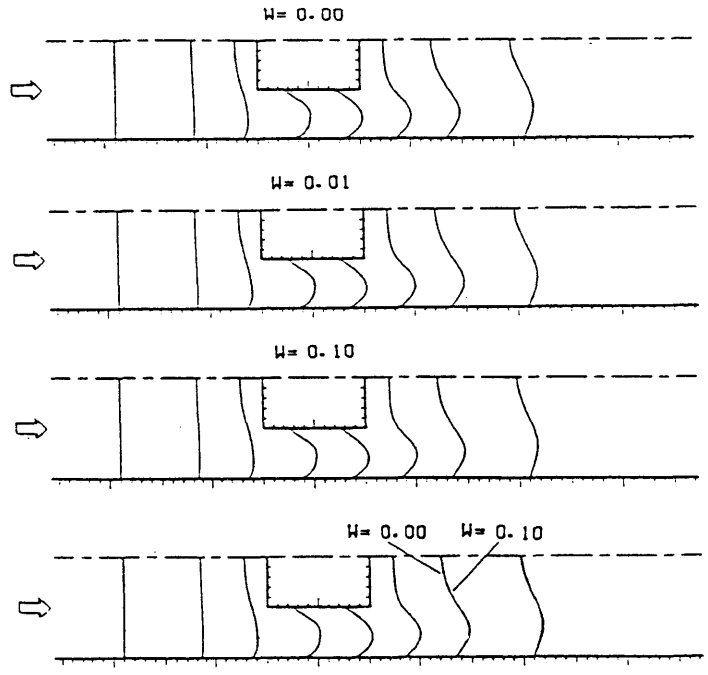

(b) Re = 50

Fig.11 Velocity distribution in viscoelastic fluids

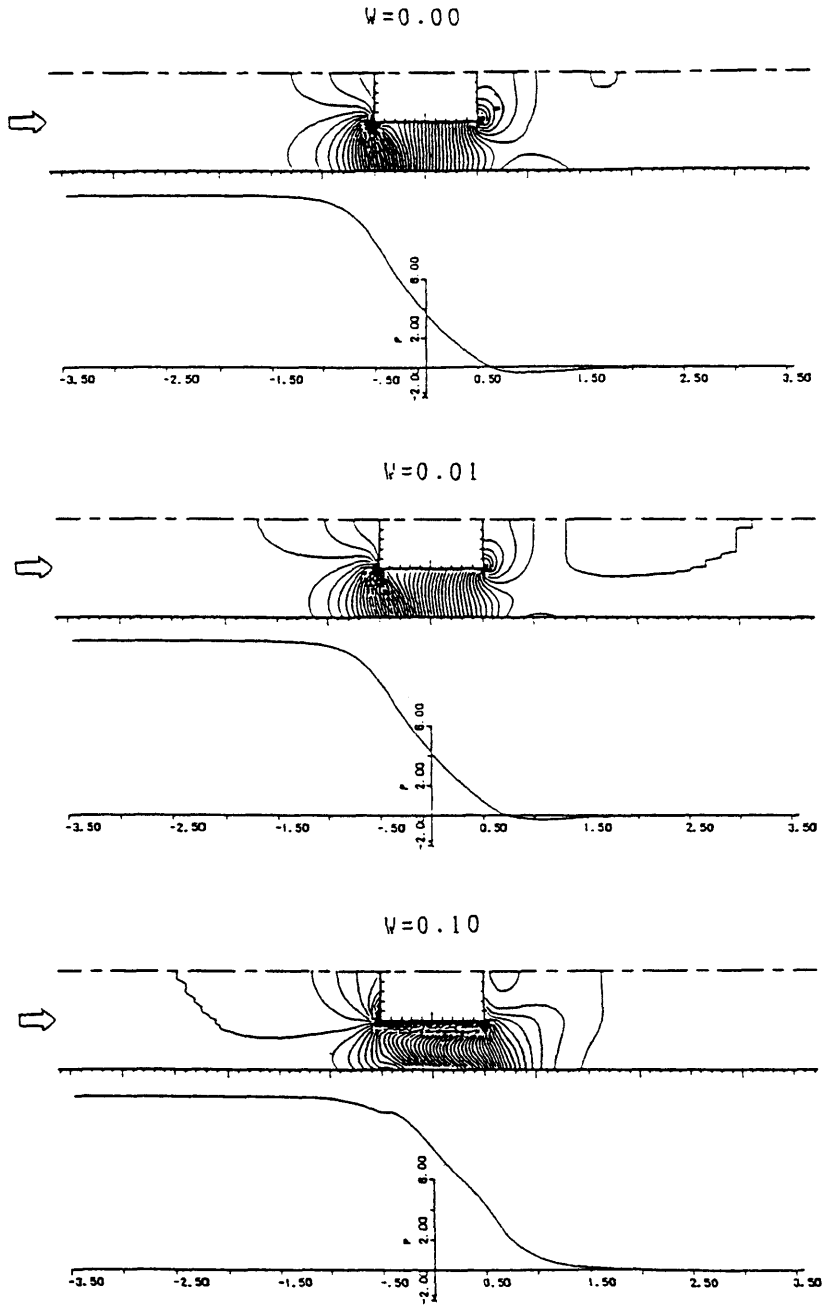

Fig.12a Pressure change in viscoelastic fluids (Re=10)

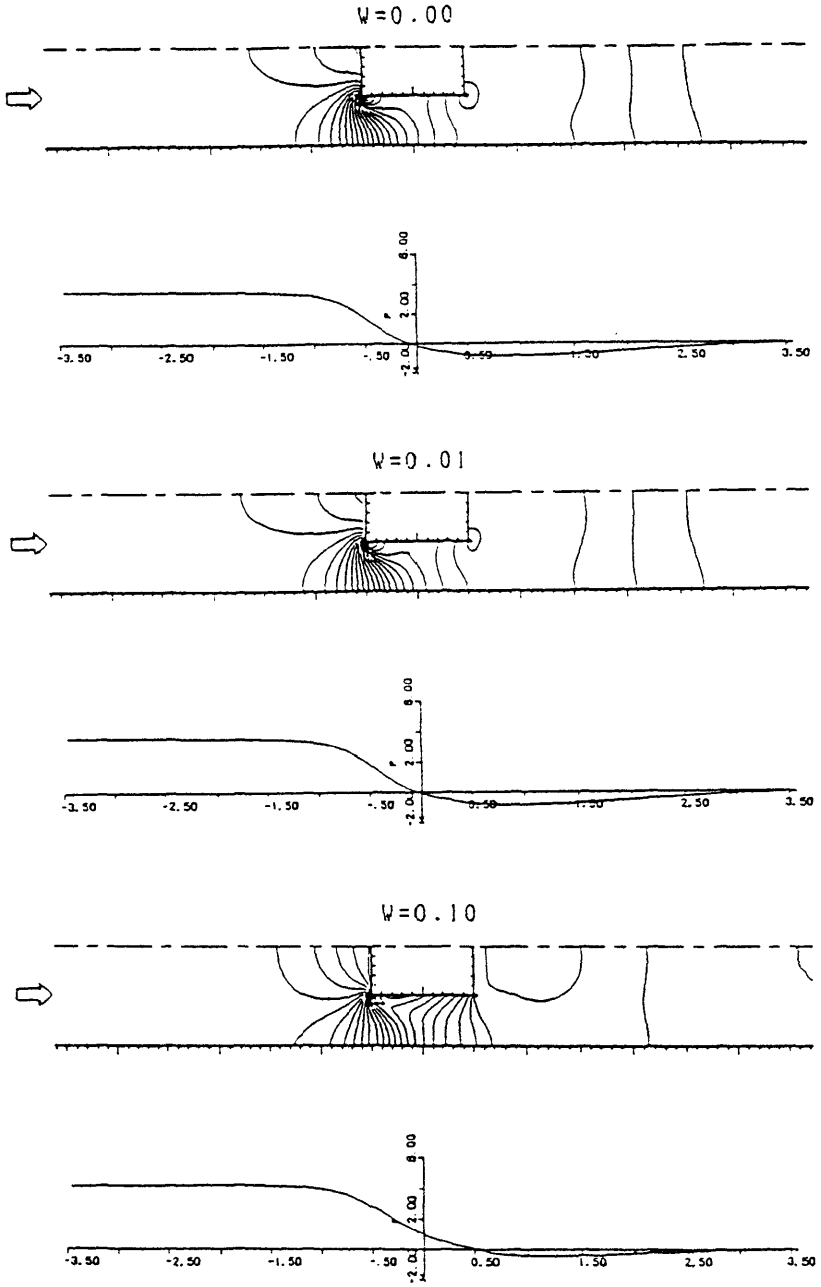

Fig.12b Pressure change in viscoelastic fluids (Re=50)

these figures, we obtained the relation of L/B and W at different Re as illustrated in Fig.13, which showed that L/B increased with an increase of Re and decreased with an increase of W. This agrees qualitatively with the conclusion in the experiment of visualization, considering that the elasticity of polymer solution increases with its concentration. Fig.11 shows the change of velocity distribution. It is found that the effect of W is less than that of Re. Fig.12 shows the pressure distribution in the flow field and the pressure drop on the channel side-wall. It was detected that the local pressure distribution changed considerably by the effect of fluid elasticity. And that, the discontinuous change of pressure drop appeared in the case that the effect of fluid elasticity was strong, e.g. Re=10 and W=0.10. This phenomenon appears on the channel side-wall of the front corner of square cylinder. Besides, its appearance moves to higher W with an increase of Re. At last, it is impossible to see it at W=0.10 in the case of Re≒50. Therefore, it can be considered that both of Re and W are concerned in this abnormality.

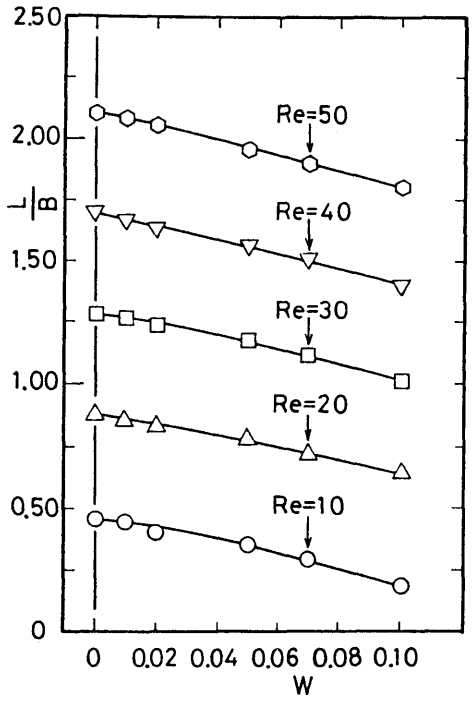

Fig.13 Length of twin-vortices in viscoelastic fluids

5. Conclusions

The two-dimensional flow field around a square cylinder moving slowly with a constant velocity along the central plane of channel was studied by the flow visualization and the numerical analysis. The effects of the channel side-wall and the fluid elasticity to the flow field were discussed. The results obtained are as follows:

(1) The expansion of streamlines in the vicinity of the square cylinder is suppressed by the approach of the channel side-wall and the length of twin-vortices in the rear of square cylinder decreases with a decrease of the ratio of the channel width to the side length of square cylinder.

(2) The fluid elasticity in viscoelastic fluids suppresses the expansion of streamlines in the rear part of the square cylinder and makes rear twin-vortices smaller. This effect of fluid elasticity increases with an increase of fluid elasticity parameters such as the polymer concentration and Weissenberg number, etc.

Acknowledgments

The authors thank to Mr.Kiyoshi Yoshida, an engineer of Fukui University, for making the experimental apparatus and drawing the figures.

References

1) J.F.Fromm & F.H.Harlow: Numerical Solution of the Problem of Vortex Street Development, *Phys. of Fluids*, 6 (1963), 975-982.

2) M.Hayashi: On the Wake Vortices behind Rectangular Cylinders at Low Reynolds Numbers, *Tech. Rep. of Kyushu Univ.*, 45 (1972), 936-942 (in Japanese).

3) Y.Matida et al.: Numerical Study of Steady Two-Dimensional Flow Past a Square Cylinder in a Channel, *J. of Phy. Soc. Japan*, 38 (1975), 1522-1529.

4) M.Tachibana: Effects of Plane Side-walls to the Flow around the Rectangular Cylinder in a Channel, *5th Symposium on Flow Visualization, ISAS Univ. of Tokyo*, (1977), 1-6 (in Japanese).

5) M.Tachibana & Y.Matsumoto: Two-Dimensional Flows around a Rectangular Cylinder Put in the Papallel Plane Side-wall Channel, *Tech. Rep. of Fukui Univ.*, 28 (1980), 129-140 (in Japanese).

6) K.Nakabayashi & T.Aoi: Numerical Analysis for Flows around an Infinitely Long Square Cylinder between Two Papallel Walls, *Trans. JSME.(B)*, 53 (1987), 49-54 (in Japanese).

7) Y.Ouwa et al: Numerical Analysis of Unsteady Two-Dimensional Flows around a Square Cylinder between Two Parallel Walls, *Trans. JSME. (B)*, 54 (1988), 277-281 (in Japanese).

8) Y. Tomita: Rheology, (*Corona Pub. Co.*, 1975) (in Japanese).

9) K.Vissmann & H.W.Beweresdorff: The Influence of Pre-shearing on the Elongational Behaviour of Dilute Polymer and Surfactant Solutions, *J. of Non-Newtonian Fluid Mech.*, 34 (1990), 289-317.

10) C.Bruce & W.H.Schwarz: Rheological Properties of Ionic and Nonionic Polyacrylamide Solutions, *J. of Polymer Sci.*, 7 (1969), 909-927.

11) T.Hasegawa: Measurement of the First Normal Stress Differences of Water and Dilute Polymer, *Trans. JSME.*, 44 (1978), 1606-1615(in Japanese).

12) K.C.Tam & C.Tiu: Steady and Dynamic Shear Properties of Aqueous Polymer Solutions, *J. of Rheology*, 33 (1989), 257-280.

13) N.Kawabata et al: A Numerical Simulation of Viscoelastic Fluid Flow in a Two-dimensional Channel (Application of Lax's Scheme to the Constitutive Equation), *Trans. JSME.(B)*, 56 (1990), 601-608 (in Japanese).